Models of the Cytochromes *b*. 2. Effect of Unsymmetrical Phenyl Substitution on Pyrrole Proton Shifts of a Series of Low-Spin (Tetraphenylporphinato)iron(III) Bis(*N*-methylimidazole) Complexes

F. Ann Walker,*[1] Virginia L. Balke, and Gregory A. McDermott

Contribution from the Department of Chemistry, San Francisco State University, San Francisco, California 94132. *Received July 9, 1981*

Abstract: In order to understand the effects of unsymmetrical substitution on the porphyrin π and metal d orbitals, we synthesized two series of tetraphenylporphyrin complexes of Fe(III) and studied their low-spin bis(*N*-methylimidazole) complexes by NMR spectroscopy. One series, the six $(p\text{-Cl})_x(p\text{-NEt}_2)_y$*TPPFe*$(N\text{-MeIm})_2^+$ complexes, have pyrrole-H resonances in the 15–19 ppm region upfield from Me_4Si. The mixed para-substituted complexes have their pyrrole-H resonances split into two to four peaks whose positions and intensities are fully consistent with the expected electron-density distribution in one of the two $3e(\pi)$ orbitals, when modified by the electron-donating and -withdrawing nature of the *p*-phenyl substituents as they are distributed for each isomer. The other series, a large number of $(m\text{- or }p\text{-Y})_1(m\text{- or }p\text{-X})_3$TPPFe$(N\text{-MeIm})_2^+$ complexes, show three pyrrole-H resonances at 90 MHz, of relative intensity 1:1:2 as the magnetic field increases when Y is more electron withdrawing than X and 2:1:1 when Y is more electron donating than X. A plot of the total spread of the pyrrole-H resonances, $\Delta\delta$, against the difference between the Hammett σ constants for X and Y, $\Delta\sigma$, is linear, with slope = 2.28 ppm. This indicates that the pattern and spread of pyrrole-H resonances depend only upon the *difference* in the electron-donating power of the substituents and not upon the *identity* of the substituents. Only two exceptions have been found to the above linear correlation: those with X = H, Y = *m*- and *p*-$NHCOCH_3$. Ortho-substituted complexes show a more complex behavior, with the pattern and spread of pyrrole-H resonances probably being a complex function of electronic, field, and axial ligand hindered rotational effects.

The cytochromes *b* are a class of low-potential heme proteins which contain noncovalently bound protoheme and appear to be present in all energy-transducing membranes.[2-5] The crystal and molecular structure of the best known of the *b* cytochromes, the water-soluble portion of proteolyzed microsomal cytochrome b_5 from calf liver, has shown that the protoheme is held in a cleft near the surface of the protein by coordination of an imidazole nitrogen of each of two histidine side chains of the protein (His 39 and 63) to the axial positions of the iron.[5,6] The orientation of the heme has recently been reevaluated[7] and found to be consistent with the predictions made from NMR studies.[8]

NMR studies of the water-soluble portion of cytochrome b_5 and the water-soluble portion of bakers' yeast flavocytochrome b_2 (called b_2 core) have long indicated a strong similarity in the heme center of these diverse members of the cytochromes *b* class and have strongly implied that b_2 core as well as b_5 has two imidazole groups from histidine side chains coordinated to the axial positions of the protoheme iron. Recently it has been shown[9-14] that not only the NMR spectra but also other spectroscopic properties (UV–visible, ESR) and the amino acid sequences of such diverse heme proteins as liver sulfite oxidase, bakers' yeast flavocytochrome b_2, and bovine erythrocyte cytochrome b_5 are very similar to those of microsomal b_5, suggesting that all of these heme proteins belong to a "novel protein superfamily" which involves the same coordination sphere for iron and similar molecular surface areas involved in the recognition of the cytochrome *c* and reductases of each protein and suggests a common evolutionary ancestor for the *b*-type cytochromes in such diverse organisms as higher animals and yeast.[14]

NMR studies of the paramagnetic Fe(III) forms of cytochromes b_5[8,15,16] and b_2[9] core, as well as the imidazole complex of methemoglobin[17] and the simple protohemin-bis(imidazole) active site in the absence of protein[18,19] have identified the hyperfine-shifted methyl resonances of the low-spin protohemin ring, and in several cases the four methyl peaks have been assigned (Table I). Similar studies of methemoglobin,[20] metmyoglobin,[21,22] leghemoglobin,[23] and cytochrome c[24] cyanides, the simple protohemin–imidazole–cyanide complex,[18,19] and the "chelated hemin"[25] cyanides have been carried out (Table I). Within each known coordination sphere (two imidazoles or one imidazole and one cyanide), the methyl resonances of the protohemin are shifted downfield (except in one case) by differing amounts depending on the specific protein or other environment, and the order also differs for the major and minor forms of those proteins which exhibit heme rotational

(1) Recipient, NIH Research Career Development Award, 1976–81.
(2) Kamen, M. D.; Horio, T. *Annu. Rev. Biochem.* **1970**, *39*, 673–700.
(3) Knaff, D. B. *Coord. Chem. Rev.* **1978**, *26*, 47–70.
(4) Cramer, W. A.; Whitmarsh, J.; Horton, P. In "The porphyrins"; Dolphin, D., Ed.; Academic Press: New York, 1979; Vol. III, pp 71–105.
(5) Mathews, F. S.; Czerwinski, E. W.; Argos, P. In "The Porphyrins"; Dolphin Ed.; Academic Press: New York, 1979; Vol. III, p 108–147.
(6) Mathews, F. S.; Argos, P.; Levine, M. *Cold Spring Harbor Symp. Quant. Biol.* **1971**, *36*, 387–395.
(7) Mathews, F. S. *Biochim. Biophys. Acta* **1980**, *622*, 375–379.
(8) Keller, R. M.; Wuthrich, K. *Biochim. Biophys. Acta*, **1980**, *621*, 204–217.
(9) Keller, R. M.; Groudinsky, O.; Wuthrich, K. *Biochim. Biophys. Acta* **1973**, *328*, 233–238.
(10) Guiard, B.; Lederer, F. *Biochim. Biophys. Acta* **1978**, *536*, 88–96.
(11) Kessler, D. L.; Rajagopalan, K. V. *J. Biol. Chem.* **1972**, *247*, 6566–6573.
(12) Guiard, B.; Lederer, F. *Eur. J. Biochem.* **1977**, *74*, 181–190.
(13) Douglas, R. H.; Hultquist, D. E. *Proc. Natl. Acad. Sci. U.S.A.* **1978**, *75*, 3118–3122.
(14) Guiard, B.; Lederer, F. *J. Mol. Biol.* **1979**, *135*, 639–650.
(15) Keller, R. M.; Groudinsky, O.; Wuthrich, K. *Biochim. Biophys. Acta* **1976**, *427*, 497–511.
(16) LaMar, G. N.; Burns, P. D.; Jackson, J. T.; Smith, K. M.; Langry, K. C.; Strittmatter, P. *J. Biol. Chem.* **1981**, *256* 6075–6079.
(17) Morishima, I.; Neya, S.; Yonezawa, T. *Biochim. Biophys. Acta* **1980**, *621*, 218–226.
(18) Frye, J. S.; LaMar, G. N., quoted in ref 19.
(19) LaMar, G. N.; Walker, F. A. In "The Porphyrins"; Dolphin, D., Ed.; Academic Press: New York, 1979, Vol. IV, p 61–157.
(20) LaMar, G. N.; Smith, K. M.; Gersonde, K.; Sick, H.; Overkamp, M. *J. Biol. Chem.* **1980**, *255*, 66–70.
(21) Mayer, A.; Ogawa, S.; Shulman, R. G.; Yamane, T.; Cavaleiro, J. A. S.; Rocha Gonsalves, A. M. d'A.; Kenner, G. W.; Smith, K. M. *J. Mol. Biol.* **1974**, 86, 749–756.
(22) LaMar, G. N.; Budd, D. L.; Smith, K. M. *Biochim. Biophys. Acta* **1980**, *622*, 210–218.
(23) Trewhella, J.; Wright, P. E. *Biochim. Biophys. Acta* **1980**, *625*, 202–220.
(24) Smith, M.; McLendon, G. *J. Am. Chem. Soc.* **1981**, *103*, 4912–4921.
(25) Traylor, T. G.; Berzinis, A. P. *J. Am. Chem. Soc.* **1980**, *102*, 2844–2846.

0002-7863/82/1504-1569$01.25/0

Table I. Protohemin Methyl Isotropic Shifts at Room Temperature for a Series of Bis(Imidazole)- and Imidazole-Cyanide-Ligated Heme Centers[a]

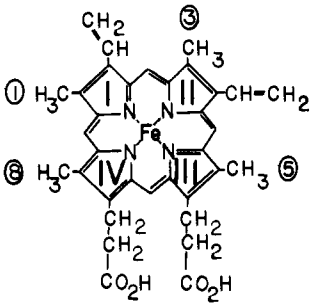

Feproto(Im)$_2$$^+$ [b] ($CDCl_3$)	pig liver cyt b_5 [d] major	pig liver cyt b_5 [d] minor	bakers' yeast cyt b_2 [e]	horse Mb(Im) [f]
−13.0 (8)[c]	−19.5 (5)[c]	−29 (3)[c]	−16.1	−36.8
−12.7 (5)	−10.7 (3)	−25 (8)	−9.3	−24.2
−10.5 (3)	−8.5 (1)	−14		−14.6
−9.8 (1)	1.0 (8)			

Feproto(CN)Im [b] CD_3OD	Feproto(CN)Im [b] Me_2SO-d_6	chelated protohemin [g] Me_2SO-d_6	whale MbCN [h]	insect HbCN (monomeric) [i] major	insect HbCN (monomeric) [i] minor	soybean leghemoglobin CN [j]	cyt c CN [k]
−15.1 (8)[c]	−13.3 (8)[c]	−18.0	−23.2 (5)[c]	−23.2 (8)[c]	−24.3 (5)[c]	−19.7 (8)[c]	−19.5 (5)
−14.6 (5)	−12.9 (5)	−16.5	−14.5 (1)	−18.3 (3)	−16.0 (1)	−17.3 (3)	−17.5 (8)
−10.4 (3)	−9.8 (3)	−15.6	−9.7 (8)			(−10.2)	−12.9 (1)
−9.7 (1)		−11.2	−6 (3)				−7.7 (3)
		−7.2					
		−4.4					
		−3.9					
		−0.9					

[a] Isotropic shifts from the positions of the methyl resonances of diamagnetic protoheme expressed in ppm, utilizing the sign convention common for paramagnetic complexes; i.e., downfield shifts are negative. [b] Reference 18. [c] Numbers in parentheses refer to methyl assignments. These assignments have been made by utilizing deuterium labeling of specific methyl groups[16,18,20,21,23] or by saturation-transfer studies of the partially oxidized ferroheme protein.[15,24] [d] References 8 and 15; assignments for "minor" species from ref 16. [e] Reference 9. [f] Reference 17. [g] Reference 23. [h] Reference 21. [i] Reference 20. [j] Reference 23. [k] Reference 24.

heterogeneity upon reconstitution.[8,15,16,20] Only by replacing the vinyls of protohemin with one acetyl group and one proton can such extremely different methyl resonance positions be produced outside the proteins.[26]

The methyl proton hyperfine shifts have been shown to be largely contact in origin.[19] and the diversity in the positions and orders of these methyl groups, as demonstrated by the data of Table I, therefore indicates differences in the unpaired electron distribution in the π obitals of the heme, depending upon its environment. It would thus appear that a given coordination sphere for iron (protoporphyrin IX plus two imidazoles, for example) is perturbed in some unique manner by placing that iron coordination sphere inside a protein. For proteins in which the active-site environment is apparently similar, such as cytochromes b_5 and b_2 core (i.e., with the heme in a cleft near the surface and with the propionic acid groups exposed to the aqueous environment[5-7]), two possible explanations as to why the protohemin methyl contact shifts differ have been suggested: (1) that protein residues press against different portions of the heme in one protein vs. those in another or in the two heme rotational forms of one protein, thereby affecting the π electron density in that part of the heme and causing a unique unpaired electron asymmetry in each protein and its heme rotational isomer,[27] and (2) that the (planar) axial imidazoles are held in prticular alignments with respect to each other and with respect to the unsymmetrical heme substituents through hydrogen bonding or other protein interactions, and thus their π orbitals may interact unequally with the d_{xz} and d_{yz} orbitals of iron.[19,24,25,28] These e-symmetry d_π metal orbitals contain three electrons in low-spin Fe(III), and although they are in principle nondegenerate because of the Jahn-Teller effect, they are averaged in energy at ambient temperatures in model compounds where axial ligands can rotate freely. When the axial ligands are constrained by the protein, this is no longer expected to be true,[29] and thus the particular angular alignment of axial ligand planes could allow different degrees of preferential interaction with one of the d_π orbitals, thus permitting unpaired electron delocalization preferentially to one of the 3e(π) porphyrin orbitals into which the unpaired electron of low-spin Fe(III) is delocalized by L→M back-bonding. Both possibilities 1 and 2 could in principle be amplified by differing strengths of hydrogen-bonding interactions of the coordinated histidine imidazoles, since stronger hydrogen-bond formation should increase the ligand field of the coordinated imidazole as it becomes more like an imidazolate anion.[30,31] All three effects may be involved in determining the redox potentials of individual cytochromes *b*.

The same explanations (1 and 2) above may be advanced to explain the NMR spectra of any ferriheme protein which contains at least one planar axial ligand, and since most heme proteins investigated so far by NMR spectroscopy contain at least one ligated histidine imidazole, it has not been possible thus far to distinguish between (1) the effect of pressure of nonbonded protein residues against the porphyrin π-electron system on unpaired-electron delocalization and (2) the exclusive effect of the orientation of the plane of the axial ligand(s) on unpaired-electron delocalization.

Model studies of the effect of restricted axial-ligand rotation (possibility 2 above) on the NMR spectra of low-spin iron(III)

(26) LaMar, G. N. In "Biological Applications of Magnetic Resonance"; Shulman, R. G., Ed.; Academic Press: New York, 1979, pp 305-343.
(27) LaMar, G. N.; Budd, D. L.; Viscio, D. B.; Smith, K. M.; Langry, K. C. *Proc. Natl. Acad. Sci. U.S.A.* **1978**, *75*, 5755-5759.
(28) Shulman, R. G.; Glarum, S. H.; Karplus, M. *J. Mol. Biol.* **1971**, *57*, 93.
(29) Horrocks, W. DeW.; Greenberg, E. S. *Mol. Phys.* **1974**, *27*, 993-999.
(30) Walker, F. A.; Lo, M.-W.; Ree, M. T. *J. Am. Chem. Soc.* **1976**, *98*, 5552-5560.
(31) Valentine, J. S.; Sheridan, R. P.; Allen, L. C.; Kahn, P. C. *Proc. Natl. Acad. Sci. U.S.A.* **1979**, *76*, 1009-1013.

porphyrins utilizing "chelated" protohemin[25] and mono-ortho-substituted (tetraphenylporphinato)iron(III)[32] have suggested that hindered rotation may be very important in determining the contact shifts of pyrrole protons or methyl groups: the "chelated" protohemin model complexes, which are a mixture of two monocyano, monoimidazole geometries which apparently differ in the angular alignment of the axial-ligand planes, have eight methyl resonances which in one case are spread over a range similar to that of metmyoglobin cyanide.[25] Likewise, mono-ortho-substituted (tetraphenylporphinato)iron(III) bis(imidazole) complexes show pyrrole-H patterns which depend upon the nature and size of the ortho substituent and the specific imidazole used.[32] It was concluded in the latter work that the observed pattern and magnitude of splitting of the pyrrole proton resonance are due to a sensitive balance of two main factors: restricted rotation of one axial ligand by the *o*-phenyl substituent and the symmetry-breaking effect of that substituent.[32]

It was not possible to separate the contributions of the *o*-phenyl substituent to restricted rotation of an axial ligand and its inherent symmetry-breaking effect[31] (which we will call its "unsymmetrical substituent effect"). We have therefore undertaken separate investigations of these two aspects. The effect of restricted rotation will be the subject of later reports. The work reported herein seeks to answer in a quantitative fashion the question: What is the effect of unsymmetrical substitution on the phenyl rings of low-spin Fe(III) tetraphenylporphyrins on the observed pyrrole proton resonance pattern, and how may this observed pattern be interpreted in terms of the π orbital(s) into which the unpaired electron is delocalized? In order to answer this question, we have prepared a large series of unsymmetrically phenyl-substituted tetraphenylporphyrin complexes of iron(III), most of which have the substituents in the meta or para positions of the phenyl rings so as not to hinder the rotation of axial ligands, and have investigated the NMR spectra of their bis(*N*-methylimidazole) complexes. *N*-Methylimidazole was chosen as the axial ligand in order to prevent the possible contribution of N–H hydrogen bonding[30,31] to the observed NMR spectra, which would complicate the interpretation of the results. In most cases the unsymmetrical complexes were of the type[33] $(Y)_1(X)_3TPPFe(N\text{-MeIm})_2^+$, but in one case, $(p\text{-Cl})_x(p\text{-Et}_2)_yTPPFe(N\text{-MeIm})_2^+$ ($x + y = 4$; $x = 0 - 4$), all six formula and structural isomers were investigated.

Though the present studies involve the effect of substituents upon the NMR shifts of pyrrole protons, the compounds involved are of a nature which cannot allow a significant amount of direct resonance coupling between the substituents and the porphyrin π system.[34] Therefore, we may also consider the unsymmetrically substituted tetraphenylporphyrins as potential models of the effect of protein residues pressing against the prophyrin π system to make the π-electron density unsymmetrical in the heme proteins.[27]

Experimental Section

Symmetrical tetraphenylporphyrins were prepared according to the method of Adler et al.[35] and purified by gravity column chromatography on silica gel (Baker chromatographic grade). Unsymmetrical tetraphenylporphyrins were prepared by a modification of this method, in which half of the mole quantity of aldehyde required for the synthesis was provided by one ortho-, or meta-, para-substituted benzaldehyde and half by a different benzaldehyde. This procedure led to an approximately statistical (1:4:2:4:4:1) distribution of isomers which usually (except for those prepared from *p*-diethylamino or any nitrobenzaldehyde) crystallized from propionic acid. All product mixtures were analyzed by TLC (Eastman Chromagram silica gel) to determine what solvent system would allow separation of the isomers. Often the best solvent mixture was found to be 70% benzene/30% petroleum ether. Only when one of the types of phenyl substituents was a polar group (OCH_3, NEt_2, CN, or NO_2) could the separation be effected, and even then, only in the case of the *p*-Cl, *p*-NEt_2 combination was it possible to separate the cis and trans isomers of the 2X, 2Y formula.[34] Small amounts of the isomers could be separated by HPLC, but because of low solubility, quantity separations were done on large gravity flow columns (3 cm × 1.5 m). Many fractions were collected and checked by TLC before combining those containing one pure isomer. The identity of the purified compounds was established by NMR spectroscopy, particularly by observing the resonance pattern of the pyrrole protons at ca. 8.8–9.0 ppm downfield from Me_4Si.[34]

Iron was inserted into the porphyrin ring by the method of Adler et al.[36] with the following modification: after the porphyrin and $FeCl_2$ were refluxed in DMF until the reaction was complete by visible spectroscopy, the solution was cooled to room temperature. An equal volume of dichloromethane was added, the mixture was then poured through ca. 500 mL of H_2O in a separatory funnel, and the CH_2Cl_2 layer was immediately drawn off without shaking. The CH_2Cl_2 layer was then reintroduced to a clean 500 mL of H_2O in the separatory funnel, shaken, and separated. This was repeated 3 additional times to remove all DMF. The dichloromethane solution was evaporated to dryness, and the sample was redissolved in a small quantity of CH_2Cl_2, poured onto a dry silica gel column (1.5 cm × 25 cm), and eluted with 10% methanol/90% CH_2Cl_2. The iron porphyrin fraction was evaporated to dryness and redissolved in CH_2Cl_2, and gaseous HCl was bubbled through to reconvert and μ-oxo dimer back to the chloroiron monomer form. The CH_2Cl_2 solutions were again evaporated to dryness.

N-Methylimidazole (Aldrich) was purified by conventional distillation. Deuteriochloroform (Merck) was used without purification. NMR solutions were ca. 0.01 M in iron porphyrin and 0.10 M in *N*-methylimidazole.

NMR spectra were run on a Varian EM-390 spectrometer operating at 90 MHz with probe temperature held stable at 33 °C. One series of NMR spectra was also run at 250 MHz on the University of California, Berkeley, NMR spectrometer; probe temperature = 21 °C.

Discussion

Effect of the Pattern of Unsymmetrical Substitution on the NMR Spectra of $TPPFe(N\text{-MeIm})_2^+$ Derivatives. The synthesis, separation, and spectroscopic investigation of the six formula and geometrical isomers of $H_2TPP(p\text{-Cl})_x(p\text{-NEt}_2)_y$[33] are reported elsewhere.[34] NMR investigations indicated that the transfer of the electronic effect of the para substituents is overwhelmingly inductive in nature, and probably includes both σ and π induction.[34] The large difference in the electronic effects of the *p*-Cl ($\sigma = 0.227$[37]) and *p*-NEt_2 ($\sigma \sim -0.83$[38]) groups is felt largely at the closest pyrrole-H position, H_a, for example in Figure 1B, and is attenuated by more than a factor of 10 at the next-closest pyrrole-H position, H_b.[34] With this background in mind we turn to the NMR spectra of the pyrrole-H region of the low-spin paramagnetic Fe(III) complexes of these six isomers, shown in Figure 1. We first note that the symmetrical complexes **1** and **6** both give single pyrrole-H resonances, as expected, with the $(p\text{-Cl})_4TPP(N\text{-MeIm})_2^+$ resonance shifted about 1.13 ppm upfield from that of $(p\text{-NEt}_2)_4TPPFe(N\text{-MeIm})_2^+$. Furthermore, the unsymmetrical compounds **2–5** have the weighted average center of their resonances at intermediate positions such that there is a linear dependence of the average isotropic shift on the number of diethylamino groups present (a downfield shift of ~0.28 ppm per *p*-NEt_2). This downfield shift is considerably smaller than the chemical shift differences between individual pyrrole-H resonances of each compound and may represent a minor dependence of either contact or dipolar shift (or both) on electronic effects of substituents.

It has been shown[19] that the major contribution to the isotropic shifts of the pyrrole-H of low-spin Fe(III) porphyrins is the contact interaction, in which unpaired electron density is delocalized from the $[d_{xz},d_{yz}]^3$ orbitals of iron into the $3d(\pi)$ filled orbitals of the porphyrin[32,39] (Figure 2a,b) by P→Fe π back-bonding. With this in mind, the pyrrole-H peaks of Figure 1 may be assigned by considering how the electronic effects of substituents should

(32) Walker, F. A. *J. Am. Chem. Soc.* **1980**, *102*, 3254–3256.
(33) Abbreviations used: NEt_2 = diethylamino; *N*-MeIm = *N*-methylimidazole; TPP = *meso*-tetraphenylporphyrin.
(34) Walker, F. A.; Balke, V. L.; McDermott, G. A., submitted for publication.
(35) Adler, A. D.; Longo, F. R.; Finarelli, J. D.; Goldmacher, J.; Assour, J.; Korsakoff, L. *J. Org. Chem.* **1967**, *32*, 476.
(36) Adler, A. D.; Longo, F. R.; Kampas, F.; Kim, J. *J. Inorg. Nucl. Chem.* **1970**, *32*, 2443–2448.
(37) Leffler, J. E.; Grunwald, E. "Rates and Equilibria of Organic Reactions"; Wiley: New York, 1963, p 173.
(38) The σ constant used for π-NEt_2 is that for *p*-NMe_2.[37]
(39) Longuet-Higgins, H. C.; Rector, C. W.; Platt, J. R. *J. Chem. Phys.* **1950**, *18*, 1174–1181.

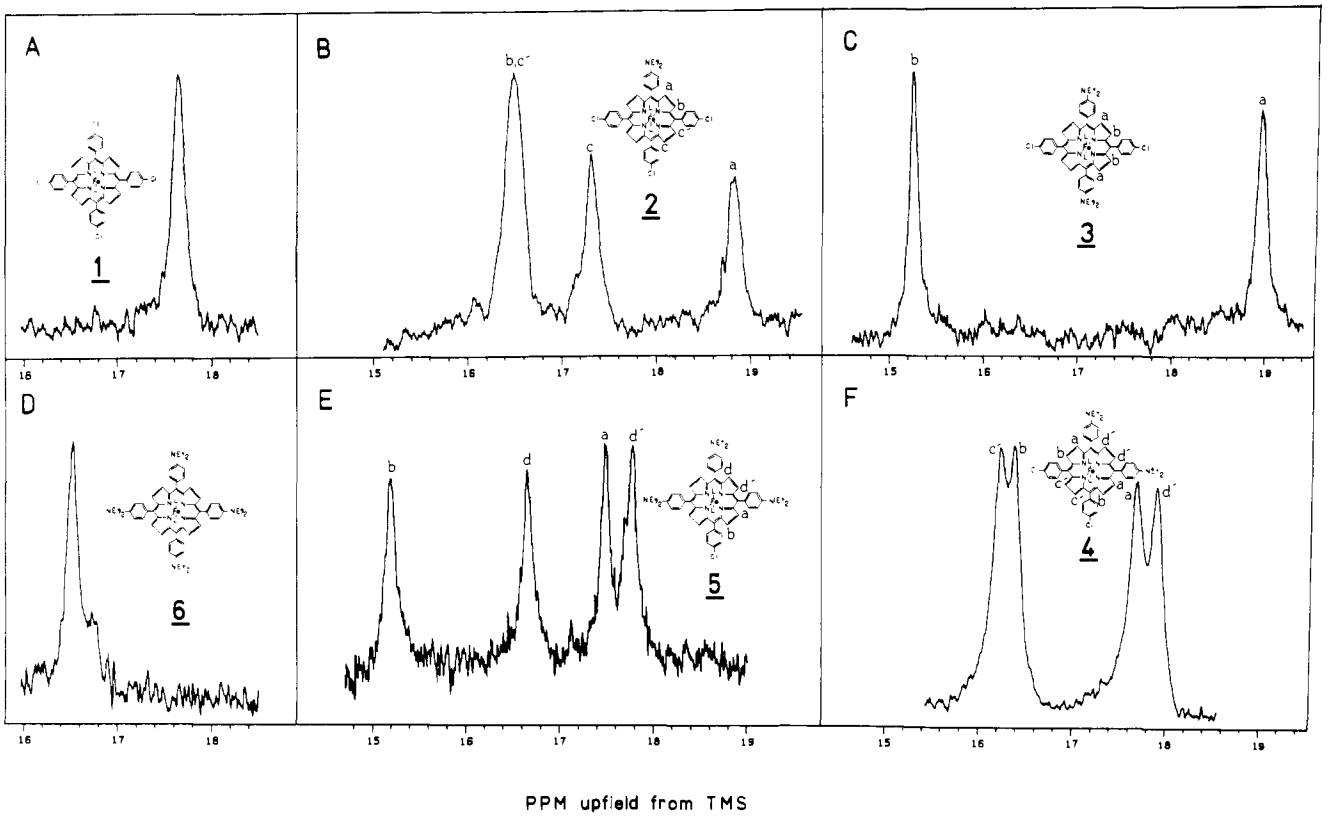

Figure 1. NMR spectra of the pyrrole-H region of the compounds of this study, recorded at 250 MHz at probe temperature (~21 °C) in $CDCl_3$ vs. Me_4Si as reference. The structures of the compounds, the types of pyrrole-H present based on molecular symmetry, and the assignments of the pyrrole-H resonances are also included.

perturb the electron density distribution in the 3e(π) orbitals.[39]

In Figure 2a,b are shown the nodal properties of the 3e(π) porphyrin orbitals,[37,32] drawn to emphasize the symmetry elements of meso-substituted porphyrins.[32,40] If these orbitals are equally populated by P→Fe unpaired electron delocalization, then the average unpaired electron density pattern of Figure 2c will be observed, and all pyrrole-H will be equivalent. This is the case for compounds **1** and **6** (Figure 1A,D). If two *p*-Cl and two *p*-NEt_2 groups are placed symmetrically on opposite phenyls, as in compound **3**, then the inductive effects of the substituents should increase the porphyrin electron density nearest the *p*-(diethylamino)phenyl groups and decrease the porphyrin electron density nearest the *p*-chlorophenyl groups.[34] Thus the original electron-density pattern found for that 3e(π) orbital which already places large electron density at those positions will receive additional density from the diethylamino substituent (compare Figure 2, a and d). Indeed, compound **3** shows the largest separation of pyrrole-H resonances found within the series. Thus we assign the upfield peak of Figure 1C to protons a and the downfield peak to protons b.

Compounds **2** and **5** may be considered to contain one electron-donating and one electron-withdrawing substituent, respectively, relative to the other three substituents present in each compound. We have already shown[34] that the effect of a *p*-phenyl substituent is largely localized, and, to a first approximation, affects only the β-pyrrole position closest to it. For compound **2** then, the increased total electron density at the symmetrically related β-pyrrole positions H_a encourages the choice of that 3e(π) orbital which has large electron density at those particular pyrrole positions as the one into which the unpaired electron will be delocalized. That is to say, introduction of one electron-donating substituent on one phenyl ring splits the degeneracy of the 3e(π) orbitals so that the one having large electron density at those

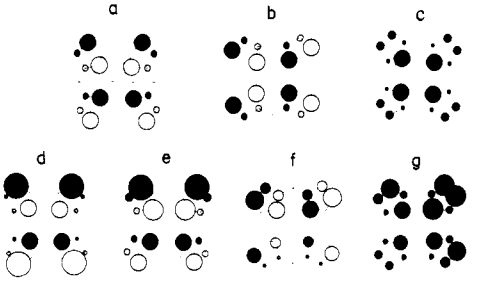

Figure 2. (a, b) Electron density and nodal properties of the porphyrin 3e(π) orbitals[31,38,39] which interact with the d_{xz} and d_{yz} orbitals of low-spin Fe(III). The light and dark shades represent orbital symmetry properties. The sizes of the circles depict the relative sizes of the squares of the atomic orbital mixing coefficients, c_i^2, for each atom, and thus represent the relative electron density at each position. (c) Average π electron density distribution of the 3e(π) orbitals of (a) and (b) remain degenerate. (d) A qualitative view of how the 3e(π) orbital of (a) is modified when electron-donating groups are placed at the upper and lower meso positions and electron-withdrawing groups at the right and left meso positions. Note that the large circles of (a) are larger and the small circles of (a) smaller in (d). (e) A qualitative view of how the 3e(π) orbital of (a) is modified when a single electron-donating group is placed on the upper meso position. Note that only the pyrrole positions and nitrogens closest to the unique meso position have increased π electron density as a result of the electron donating substituent. (f) A qualitative view of how the 3e(π) orbital of (b) is modified when a single electron-withdrawing group is placed on the lower meso position. Note again that only the pyrrole positions and nitrogens closest to the unique meso position have decreased π electron density as a result of this unsymmetrical substitution pattern. (g) Our proposed view of the π electron density distribution when two electron-donating substituents occupy adjacent (upper and right hand) meso positions, and thus perturb the average π electron distribution shown in (c).

pyrrole positions closest to the unique phenyl is shifted to higher energy and its former partner to lower energy. Ligand-to-metal π back-bonding is expected to occur with the higher-energy of the two now nondegenerate 3e(π) orbitals. Thus the pyrrole

(40) The 3e(π) orbitals as presented here are linear combinations of those originally proposed,[38] since the substitution pattern of the *meso*-tetraphenylporphyrins of this study dictates symmetry planes passing through meso positions.

positions closest to the electron-donating phenyl group will have a particularly large unpaired electron density, leading to a larger contact shift. Therefore, for compound **2** the pyrrole proton peak furthest upfield from Me_4Si is due to the protons at the pyrrole position H_a closest to the unique phenyl. Because of the electron distribution in the $3e(\pi)$ orbitals, the next most upfield pyrrole peak must be due to the pyrrole protons furthest away from the unique phenyl, H_c for **2** and the most downfield pyrrole peak (twice as intense as each of the others) to the remaining four pyrrole protons (H_b and H_c' for **2**). We may thus draw the approximate unpaired electron-density distribution of **2** as shown in Figure 2e, and by analogy, that of **5** as shown in Figure 2f.

At 60 MHz, the lowest field pyrrole-H peak of **2** and the highest field pyrrole-H peaks of **5** appear as singlets of area 2 relative to each of the other peaks present, but at 250 MHz that of **5** separates into two resonances, each of relative area 1, and that of **2** broadens. Thus to a higher level of approximation, the electronic effect of one unique para-substituted phenyl group has a minor effect on the next most adjacent pyrrole position such that it becomes slightly inequivalent to its $3e(\pi)$ symmetry-related partner. Thus we assign the resonances of complex **2** (Figure 1B) as (c', b), c, and a in order of increasing upfield shift and those of complex **5** (Figure 1E) as b, d, a, d' in the same order.

Compound **4** appears to use the $3e(\pi)$ orbitals of Figure 2a,b equally so that the only factor modifying the electron-density distribution from that of Figure 2c is the inductive effect of the *p*-(diethylamino)phenyl vs. *p*-chlorophenyl groups, as shown in Figure 2g. Thus to a first approximation there should be two pyrrole-H resonances, one due to pyrrole-H adjacent to *p*-(diethylamino)phenyl groups and one due to those adjacent to *p*-chlorophenyl groups, as is the situation at 60 and 90 MHz. However, to a higher approximation, if the inductive effect is felt to a minor extent at the next nearest pyrrole-H position, then each of the pyrrole-H resonances should split into two at higher magnetic field. Such is the case at 250 MHz (Figure 1F), and we thus assign the pyrrole-H resonances to protons c', b, a, and d' in order of increasing upfield shift.

The patterns of pyrrole-H resonances observed for the unsymmetrical complexes **2–5** and the assignments of those resonances on the basis of expected perturbation of the electron-density distribution in the $3e(\pi)$ orbitals as a function of the pattern of unsymmetrical substitution demonstrate clearly the importance of molecular symmetry in controlling the distribution of unpaired electron density in the porphyrin ring. Since nature invariably chooses to use the unsymmetrical protoporphyrin IX ring system or some chemical modification of it which is more electronically asymmetric (such as heme *a*), an important consideration in explaining the physical properties of the heme proteins must be the role of this unsymmetrical distribution of substituents. The series of compounds **1–6** clearly demonstrates how unsymmetrical substitution of groups of different electronic character affects one such physical property, the NMR spectra of the paramagnetic low-spin Fe(III) complexes. Investigations of redox potentials, ESR and electronic spectra, etc., of **1–6** are in progress.

Effect of the Nature of the Substituent on the NMR Spectra of Unsymmetrical TPPFe(*N*-MeIm)$_2^+$ Complexes. We now wish to quantify the manner in which the pattern of pyrrole-H resonances depends upon the electronic properties of the substituents. For this purpose a series of unsymmetrical Fe(III) tetraphenylporphyrins were prepared, each of which is of the type $FeClTPP(X)_3(Y)_1$, where X and Y are a series of substituents placed on the ortho, meta, or para position of the phenyl rings.

In Figure 3 are shown the NMR spectra of the pyrrole-H region of the bis(*N*-methylimidazole complexes of a series of monosubstituted derivatives (X = H) of FeClTPP, where one phenyl ring contains a single *o*-, *m*-, or *p*-NO_2, OCH_3, or NH_2. Also given in Figure 3 are the Hammett σ constants[37] for each substituent. The spectra of Figure 3 were recorded at 90 MHz, and thus differentiation between pyrrole-H types b and c' or a and d' (Figure 1) is not observed.

The mono-meta- and para-substituted derivatives of Figure 3, except for the acetamido-substituted complexes, show pyrrole-H

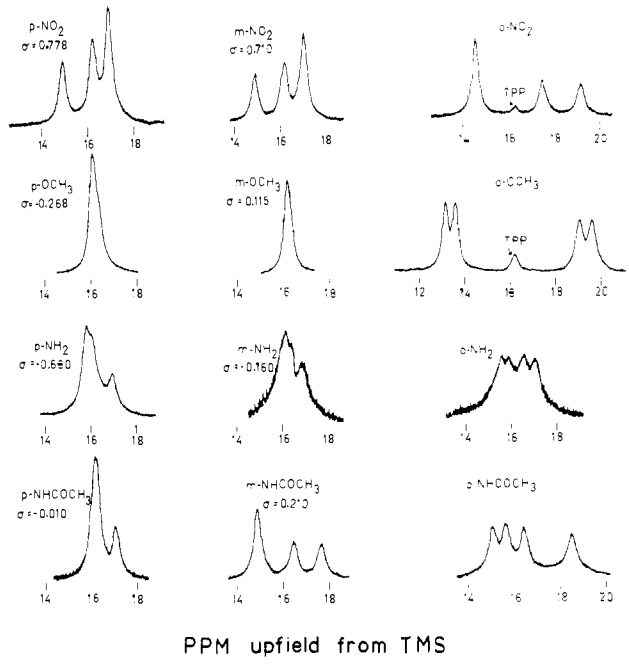

Figure 3. NMR spectra of the pyrrole-H region of a series of low-spin Fe(III) complexes of FeClTPP(*p*-, *m*-, or *o*-Y)$_1$ with *N*-methylimidazole, recorded at 90 MHz in $CDCl_3$, with Me_4Si as reference. Temperature = 33 °C. Several of the ortho-substituted derivatives contain a small amount of the symmetrical TPPFe(*N*-MeIm)$_2^+$ (marked as "TPP").

peak patterns which are fully consistent with the electronic properties of the single substituent: a *m*- or *p*-NO_2 group (large positive σ value) leads to a "1,1,2" pyrrole peak intensity pattern, fully consistent with electron delocalization into the $3e(\pi)$ orbital shown in Figure 2f, while a *p*-NH_2 group (large negative σ value) produces a "2,1,1" peak intensity pattern, consistent with electron delocalization into the $3e(\pi)$ orbital of Figure 2e. The *p*-OCH_3 group produces an unsymmetrical resonance which has a shoulder on the upfield side (small negative σ value). The *m*-NH_2 group produces a larger splitting than does the *p*-OCH_3 group, an effect which is not yet understood. The *m*-OCH_3 group provides too small an asymmetry in the π electron density to favor one orbital over the other, and thus the unpaired electron distribution is symmetrical (Figure 2c). Thus the splitting of the pyrrole-H resonance depends not only upon lowering the symmetry of the porphyrin ring but also upon the electronic properties of the groups responsible for the lowered symmetry. The mono-*m*- and *p*-acetamido groups are clearly anomalous (Figure 3). They have much larger spreads of the pyrrole-H resonances than their Hammett σ constants would have predicted by comparison to the NO_2, OCH_3, and NH_2 groups. This fact will be discussed further below.

If X and Y are both allowed to vary, a wide range of electronic asymmetry is possible. We have found that, except for acetamido groups, whenever three substituents are electron donating in comparison to the fourth, then a "1,1,2" pyrrole-H intensity pattern is observed whereas the reverse pattern ("2,1,1") is observed whenever three substituents are electron withdrawing in comparison to the fourth, *irrespective of the identity of the substituents*. In order to quantify this effect, we have plotted in Figure 4 the difference in isotropic shift ($\Delta\delta$) between the peak of area "2" and the most extreme peak of area "1" *vs.* the *difference* in Hammett σ constant ($\Delta\sigma = \sigma_Y - \sigma_X$)[37,41] between the two types of substituents present. Those compounds which have a "1,1,2" pyrrole-H peak-intensity pattern have a positive value of $\Delta\delta$ and a positive value of $\Delta\sigma$. As can be seen from Figure 4, an excellent correlation[41] exists, with slope = 2.28 ppm. Thus the spread of pyrrole-H resonances depends only upon the *difference* in σ constant of the two types of substituents and not upon

(41) The linearity of the plot is significantly better when σ[37] rather than σ^+[42,43] is used, again indicating that resonance effects are minor.

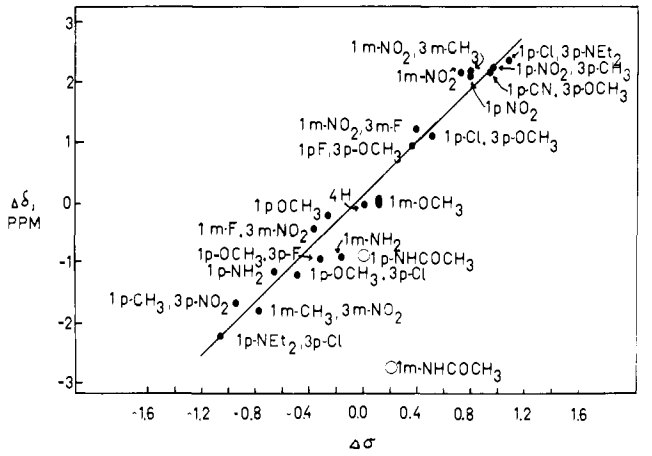

Figure 4. Plot of the separation between highest and lowest field pyrrole-H resonances vs. the difference in Hammett σ constant[36,37] for the two types of substituents involved in the $[(N\text{-MeIm})_2\text{FeTPP(X)}_3\text{(Y)}_1]^+\text{Cl}^-$ complexes.

the *sum* of σ constants of all substituents present: Consider the similarity in the pyrrole-H peak spread of the 1 *p*-F, 3 *p*-OCH_3 ($\Delta\sigma = 0.330$; $\sum\sigma = -0.742$[37]) and 1 *m*-NO_2, 3 *m*-F ($\Delta\sigma = 0.373$, $\sum\sigma = 1.721$[37]) compounds.

The only exceptions to the correlation between $\Delta\sigma$ and $\Delta\delta$ found to date are the *p*- and *m*-$NHCOCH_3$ groups ($\Delta\sigma = -0.010$ and 0.210,[42] respectively), which have much larger values of $\Delta\delta$ than their $\Delta\sigma$ values would predict (Figure 4, large open circles), indicating apparent σ constants of −0.5 and −1.3, respectively. Their correlation with the other substituents of Figure 4 is not improved if σ^+ or other reasonable types of σ constants[42,44] are used. Since the N-bound amide has been a common connecting group for many model compounds including the "picket-fence" porphyrin[45] and various "side arm"[32,45-47] or "tailed"[48,49] porphyrins, further studies are under way to elucidate the reasons for the unique pattern of pyrrole-H peaks observed for these compounds.

Although the spread of the pyrrole-H resonances does not correlate with the sum of the σ constants of the substituents, the weighted average center of the group of resonances does appear to depend slightly upon the sum of the σ constants. An upfield shift is observed as $\sum\sigma$ becomes more positive, as was mentioned for the *p*-NEt_2 and *p*-Cl isomers above. However, at $\sum\sigma > 1.0$ (i.e., mainly *m*- or π-NO_2-containing compounds) the dependence appears to break down or even reverse. The implications of this observation and the temperature dependence of the resonances for individual compounds are being investigated further.

For selected ortho substituents, the pattern of pyrrole-H resonances observed in Figure 3 is considerably more difficult to interpret. The pattern of shifts observed is probably a complex function of contributions[50] due to (1) the inductive effect of that substituent, (2) the direct field effect of the substituent due to direct overlap with the porphyrin π system, and (3) restricted rotation of one of the axial ligands due to steric interference between the ligand and the ortho substituent.[32] Studies are under way to evaluate the importance of each of these contributions.

Finally, we might point out again the ways in which such model complexes may be used to gain detailed quantitative information concerning the electronic structure of the heme proteins. (a) The electronic effects of substituents are transferred to the filled $3e(\pi)$ "reporter" orbitals by purely inductive interactions and thus could be thought of as being similar to the effect of adding or subtracting electron density to a particular portion of the porphyrin π system by the pressure[27] (or π complexation) of electron-rich or electron-poor protein residues. These model compounds thus show us the nature of the molecular orbital of natural hemins and ferriheme proteins when such protein residues press against the π system near one or more meso position. Later studies will examine the detail the effect of pyrrole substitution on the nature of the π molecular orbital. (b) The lowering of the symmetry of tetraphenylporphyrin by unsymmetrical substitution of the phenyl rings is also a model of what should happen if the axial ligands are prevented from rotating about their Fe–N bonds so that their molecular planes lie through the same opposite meso positions (Compound **3**, Figure 2d) or through perpendicular opposite meso positions (Figure 2c). Work in progress is aimed at producing compounds thus hindered in axial ligand rotation capability.

Acknowledgment. The financial support of NSF (CHE-79-18217) and NIH RCDA (5 K04 GM 00227) are gratefully acknowledged. We thank Dr. Robert Lundin and Mabry Benson for use of the NMR facilities of the U.S. Department of Agriculture, Berkeley, CA, for part of this work and Dr. Yitmin Liang for running the 250-MHz NMR spectra at University of California, Berkeley. Elaine Pico prepared the mono-*p*-OCH_3 derivative.

Registry No. 1, 80631-17-0; **2**, 80641-63-0; **3**, 80641-64-1; **4**, 80641-65-2; **5**, 80641-66-3; **6**, 80641-67-4; $(p\text{-NO}_2)\text{H}_3\text{TPPFe}(N\text{-MeIm})_2^+$, 80641-68-5; $(m\text{-NO}_2)\text{H}_3\text{TPPFe}(N\text{-MeIm})_2^+$, 80641-69-6; $(o\text{-NO}_2)\text{H}_3\text{TPPFe}(N\text{-MeIm})_2^+$, 80641-70-9; $(p\text{-OCH}_3)\text{H}_3\text{TPPFe}(N\text{-MeIm})_2^+$, 80641-71-0; $(m\text{-OCH}_3)\text{H}_3\text{TPPFe}(N\text{-MeIm})_2^+$, 80641-72-1; $(o\text{-OCH}_3)\text{H}_3\text{TPPFe}(N\text{-MeIm})_2^+$, 80641-73-2; $(p\text{-NH}_2)\text{H}_3\text{TPPFe}(N\text{-MeIm})_2^+$, 80641-74-3; $(m\text{-NH}_2)\text{H}_3\text{TPPFe}(N\text{-MeIm})_2^+$, 80641-75-4; $(o\text{-NH}_2)\text{H}_3\text{TPPFe}(N\text{-MeIm})_2^+$, 80641-76-5; $(p\text{-NHCOCH}_3)\text{H}_3\text{TPPFe}(N\text{-MeIm})_2^+$, 80641-77-6; $(m\text{-NHCOCH}_3)\text{H}_3\text{TPPFe}(N\text{-MeIm})_2^+$, 80641-78-7; $(o\text{-NHCOCH}_3)\text{H}_3\text{TPPFe}(N\text{-MeIm})_2^+$, 80641-79-8; $(m\text{-NO}_2)(m\text{-CH}_3)_3\text{TPPFe}(N\text{-MeIm})_2^+$, 80641-80-1; $(p\text{-NO}_2)(p\text{-Me})_3\text{TPPFe}(N\text{-MeIm})_2^+$, 80641-81-2; $(m\text{-CH}_3)(m\text{-NO}_2)_3\text{TPPFe}(N\text{-MeIm})_2^+$, 80641-82-3; $(p\text{-CH}_3)(p\text{-NO}_2)_3\text{TPPFe}(N\text{-MeIm})_2^+$, 80641-83-4; $(m\text{-F})(m\text{-NO}_2)_3\text{TPPFe}(N\text{-MeIm})_2^+$, 80641-84-5; $(p\text{-F})(p\text{-OCH}_3)_3\text{TPPFe}(N\text{-MeIm})_2^+$, 80641-85-6; $(p\text{-OCH}_3)(p\text{-F})_3\text{TPPFe}(N\text{-MeIm})_2^+$, 80641-86-7; $(p\text{-Cl})(p\text{-OCH}_3)_3\text{TPPFe}(N\text{-MeIm})_2^+$, 80641-87-8; $(p\text{-OCH}_3)(p\text{-Cl})_3\text{TPPFe}(N\text{-MeIm})_2^+$, 80641-88-9; $\text{H}_4\text{TPPFe}(N\text{-MeIm})_2$, 52155-25-6.

(42) Swain, C. G.; Lupton, E. C. *J. Am. Chem. Soc.* **1968**, *90*, 4328–4337.
(43) Brown, H. C.; Okamoto, Y. *J. Am. Chem. Soc.* **1957**, *79*, 1913–1917; **1958**, *80*, 4979–4987.
(44) Dayal, S. K.; Ehrenson, S.; Taft, R. W. *J. Am. Chem. Soc.* **1972**, *94*, 9113–9122.
(45) Collman, J. P.; Gagne, R. R.; Reed, C. A., Halbert, T. R.; Lang, G.; Robinson, W. T. *J. Am. Chem. Soc.* **1975**, *97*, 1427–1439.
(46) Walker, F. A.; Benson, M. *J. Am. Chem. Soc.* **1980**, *102*, 5530–5538.
(47) Bobrik, M. A.; Walker, F. A. *Inorg. Chem.* **1980**, *19*, 3383–3390.
(48) Mashiko, T.; Marchon, J.-C.; Musser, D. T.; Reed, C. A.; Kastner, M. E.; Scheidt, W. R. *J. Am. Chem. Soc.* **1979**, *101*, 3653–3655.
(49) Collman, J. P.; Brauman, J. I.; Doxsee, K. M.; Halbert, T. R.; Bunmenberg, E.; Linder, R. E.; LaMar, G. N.; Del Gaudio, J.; Lang, G.; Spartalian, K. *J. Am. Chem. Soc.* **1980**, *102*, 4182–4192.
(50) Charton, M. *Prog. Phys. Org. Chem.* **1971**, *8*, 235–317.